


## Predictive modeling of concrete strength utilizing recycled materials: a DOE methodology

Anandraj Amalraj<sup>1</sup> , Baskar Neelakandan<sup>2</sup>, Vijayabaskaran Selvarajan<sup>2</sup>

<sup>1</sup>Saranathan College of Engineering Department of Civil Engineering, Venkateswara Nagar, Panjappur, Thiruchirappalli, Tamilnadu, India.

<sup>2</sup>Saranathan College of Engineering, Department of Mechanical Engineering, Venkateswara Nagar, Panjappur, Thiruchirappalli, Tamilnadu, India.

e-mail: araj1988@gmail.com, baskamaresh@yahoo.co.in, vijayrec76@gmail.com

---

### ABSTRACT

The DOE methodology was applied to identify the best combination of variables-Recycled Aggregate (RA), Aluminium Ash dross (AAD), and Magnesium oxide dross (MOD)-to enhance concrete's mechanical properties. Utilising the Response Surface Methodology's Central Composite Design (CCD), the study examined four variables: the concrete's split tensile and compressive strengths at 14 and 28 days. ANOVA was used to test regression models for these factors, with the results displayed in a Pareto chart for visualization. The impact of each independent variable was evaluated, and second-order polynomial equations were devised to represent the models obtained. The findings suggested a positive contribution from the inclusion of RA, AAD, and MOD to improve mechanical properties, though higher levels of their inclusion led to reduced strength. Through surface plots, Pareto charts, and regression analysis, it was revealed that Recycled Aggregate and AAD were the most significant factors distressing compressive strength (CS) and split tensile strength (STS) at both 14 and 28 days. Validation tests were similar to predicted results for both compressive strength and split tensile strength, signifying the consistency of these models in predicting strength properties based on the selected variables.

**Keywords:** Recycled aggregate; Aluminium ash dross; Magnesium oxide dross; Analysis of variance; Pareto chart; Contour plot.

---

### 1. INTRODUCTION

Recycling stands as a remarkable method for handling construction waste, effectively reducing waste volume and limiting the exploitation of natural resources to protect and restore our environment. There are various methods available for recycling. Addressing this pressing issue, specific building waste like waste concrete aggregate can be recycled multiple times, contributing to fresh projects and initiatives [1]. The majority of pozzolanic materials are actually industrial by-products, such as blast furnace slag, rice husk ash and others. Surprisingly, there hasn't been extensive research conducted on producing, engineering, and optimizing purposefully designed pozzolanic materials envisioned for use in conjunction with Portland cement [2].

The utilization of RA instead of natural aggregates (NA) in concrete production has the potential to contribute to practical engineering's sustainable development [3]. This approach has undergone numerous investigations over the past few decades to assess the feasibility of incorporating RCA as substitute materials in concrete mixes [4, 5]. Aluminium dross, is among the residual by-products originating from aluminium refining and smelting processes. Its primary components encompass aluminium, aluminium oxides, and diverse salts in varying compositions [6]. The most effective proportion of recycled aggregates to natural aggregates is at a 50% mixing ratio. Under either air curing or painting conditions, the highest levels of compressive strength and tensile strength were achieved after twenty eight days curing [7]. The inclusion of RA may effect in a slight decrease in concrete compressive strength and is preferable to using recycled coarse aggregate alone or both fine and coarse aggregates together [8].

The utilization of construction and demolition debris as a substitute for coarse aggregates in concrete, focusing on workability, revealed a notable adverse reduction on workability when recycled aggregate (RA) was employed [9]. In comparison to the reference concrete, the addition of steel fibre and recycled aggregate improved the mechanical strength and changed the fracture process [10]. In concrete containing Recycled Concrete Aggregate (RCA), the strength continues to increase beyond the 28-day curing period. Conversely, in concrete containing Recycled Brick Aggregate (RBA), the strength development significantly decelerates after the initial 28 days of curing [11]. The CS of Alkali Activated Slag-Recycled Aggregate concrete showed a rise from 35.20 MPa at twenty eight days to 37.52 MPa at 365 days. In contrast, Alkali Activated Slag-Natural Aggregate concrete maintained a nearly consistent strength of 40 MPa at both 28 and 365 days [12]. The concrete comprising 100% Recycled Concrete Aggregate (RCA) combined with 10% Steel Fiber (SF) demonstrated superior flexural fatigue performance compared to concrete consisting of 100% coarse natural aggregate [13]. The concrete's compressive strength declines from 30.85 MPa to 17.58 MPa as the percentage of recycled aggregate rises from 0% to 100%. However, the incorporation of silica fume results in a subsequent increase in concrete compressive strength to 29.2 MPa for samples containing 100% recycled aggregate [14]. The replacement of Recycled concrete aggregate significantly impacts the stress-strain curves of RCA. The stress-strain curves of RCA reveal an elevation in the maximum strain and a considerable reduction in ductility, particularly evident in their descending segment [15]. Mechanical and durability properties of a concrete blend that includes 10% AAD and 15% fly ash, and 20% quarry dust surpass those of standard concrete [16]. The flexural and compressive strengths of RPC, when cured for 1 day, exhibit a decrease corresponding to the escalating amounts of secondary aluminum ash, with reduction rates ranging from 0% to 18.7% and 0% to 19.3%, respectively [17].

Concrete manufactured with a 30% replacement of Al dross encounters an increased reduction in flexural strength caused by uneven dispersal of hydration products within the concrete, particularly in warm climate circumstances [18]. The increase in Aluminium ash dross substances leads to a reduction in compressive strength. As the proportions of AAD rise, void formation becomes apparent in the AAD mortar mix, consequently leading to decreased compressive strength [19]. Incorporating Secondary aluminium ash (SAA) can enhance the mechanical strengths of RPC by elevating its activity and diminishing the associated porosity. The flexural and compressive strengths of Reactive Powder Concrete exhibit increments corresponding to the escalating rates of SAA, with growth rates ranging from 0% to 26.3% [20]. In order to study how independent factors affect results while conducting a negligible number of tests, a precise and numerical method called Design of Experiments (DOE) utilizing Response Surface Methodology (RSM) was employed. Statistical study using Central Composite Design (CCD) combined with RSM was performed in order to identify the best combination of variable elements (RA, AAD, and MOD) and evaluate their effect on compressive strength and split tensile strength. Magnesium oxide dross, aluminium ash dross, and recycled aggregate weight proportions were the independent variables taken into account in this analysis.

## 2. RESPONSE SURFACE METHODOLOGY

RSM encompasses a collection of mathematical methods utilized to enhance and optimize the efficiency of a system, process, or product. RSM serves to examine the relationship among multiple input parameters (factors) and the resulting output retort. CCD stands as a prevalent experimental design methodology within RSM, effectively employed to model and analyse the response surface. It serves as a mathematical and scientific tool to resolve scenarios where numerous influential variables significantly affect the final outcomes [21].

The Response Surface Methodology effectively leverages the correlation among multiple independent variables when the resulting parameters are notably impacted by numerous factors. CCD was used to study the effects of mix influences, precisely RA ( $y_1$ ), AAD ( $y_2$ ), and MOD ( $y_3$ ), on the CS and STS of concrete. The autonomous variables were RA ( $y_1$ ), AAD ( $y_2$ ), and MOD ( $y_3$ ), the computed response includes compressive strength  $fcs_{14}$ ,  $fcs_{28}$  and split tensile strength  $fsts_{14}$ ,  $fsts_{28}$ . The factors and variable levels for the four retorts are detailed

**Table 1:** Levels of variables.

VARIABLES	MINIMUM (%)	MAXIMUM (%)
Recycled aggregate	0	100
Aluminium ash dross	0	30
Magnesium oxide dross	0	30

**Table 2:** Combinations obtained from RSM model.

MIX	RA (%) ( $y_1$ )	AAD (%) ( $y_2$ )	MOD (%) ( $y_3$ )	COARSE AGGREGATE ( $\text{kg/m}^3$ )	FINE AGGREGATE ( $\text{kg/m}^3$ )	CEMENT ( $\text{kg/m}^3$ )
RAMD01	0	0	30	1218	646	410
RAMD02	0	30	30	1218	646	287
RAMD03	50	15	15	609	646	287
RAMD04	50	15	40	609	646	238
RAMD05	50	15	15	609	646	287
RAMD06	50	15	15	609	646	287
RAMD07	0	15	15	1218	646	287
RAMD08	100	15	15	0	646	287
RAMD09	100	0	0	0	646	410
RAMD10	50	40	15	609	646	238
RAMD11	0	30	0	1218	646	287
RAMD12	50	15	15	609	646	287
RAMD13	100	0	30	0	646	287
RAMD14	50	15	0	609	646	349
RAMD15	0	0	0	1218	646	410
RAMD16	100	30	0	0	646	287
RAMD17	50	0	15	609	646	349
RAMD18	50	15	15	609	646	287
RAMD19	50	15	15	609	646	287
RAMD20	100	30	30	0	646	164

in Table 1. In order to evaluate the impact of RA, AAD, and MOD on the strength properties of concrete, a three-factor CCD technique was implemented on 20 different mixes as shown in Table 2.

The optimal response was identified through a regression equation involving linear, collaborating, and quadratic constants. A set of 20 trials obtained from RSM was utilized for this trial, and Table 2 presents the configuration of mixes in these trials.

### 3. MATERIALS AND METHODS

This examination utilized OPC grade 53, defined by IS 12269-2013, with a sp. gr of 3.1 and an initial setting time of 35 minutes. The mix comprised 20 mm recycled coarse aggregate with a sp.gr of 2.3 and fine aggregate having a specific gravity of 2.67, conforming to zone II as per IS 10262-2019. The study incorporated Aluminium ash dross, also recognized as black dross, derived from an aluminium rolling mill, possessing a specific gravity of 2.6. Similarly, Magnesium oxide dross, a residual material from magnesium production or refining, was used, having a specific gravity of 3.7. A nominal concrete mix was created to yield M25 grade concrete, per IS 10262-1982. The water-to-binder ratio was calculated to be 0.46 and the binder to aggregate ratio to be 1:1.65:3.08. In the case of M25 grade concrete, trial mixes were devised by substituting portions of the coarse aggregate and cement with aluminium ash dross, magnesium oxide, and recycled aggregate, respectively, at varying replacement levels. A total of 20 trial mixes were created, and Table 2 presents the quantities of different materials needed to produce 1 m<sup>3</sup> of M25 grade concrete based on these trial mixes. The concrete mixture was placed into a 150 × 150 × 150 mm cubic mould for conducting the compressive test, while cylindrical moulds measuring 30 cm in height and 15 cm in diameter were utilized for the split tensile strength test. Following the casting process, the concrete samples were left in the moulds for a full day to dry. For the purpose of conducting experiments, a total of sixty concrete cube specimens and sixty cylindrical specimens were constructed. Three samples for each blend were tested after 14 and 28 days, respectively. The representative concrete strength was determined by averaging the strength values of the three samples. The concrete specimens were taken out of the moulds after fourteen and twenty-eight days of curing, and their compressive and split tensile strengths were measured with a 100 kN Compression Testing Machine (CTM).

## 4. RESULTS AND DISCUSSION

### 4.1. Compressive strength

The findings, depicted in Figure 1, revealed that incorporating RA, AAD, and MOD improved the concrete's strength properties. Figure 1 illustrates the CS characteristics of the concrete mixture at 14 and 28 days of age. The research discovered the impact of using RA as a partial substitute for coarse aggregate and AAD and MOD as partial replacements for cement on the concrete's CS. The utilization of RA, AAD, and MOD boosted the concrete's compressive strength. However, beyond a specific proportion, increasing the amount of RA, AAD, & MOD resulted in a decline in the concrete's strength. The highest CS at fourteen and twenty eight days, reaching 32.14 N/mm<sup>2</sup> and 34.80 N/mm<sup>2</sup>, respectively, were achieved with a concrete specimen featuring 50% recycled aggregate replacement and 15% cement replacement by AAD and MOD. Yet, the compressive strength declined when RA inclusion exceeded 50% [22]. The decrease in strength can be ascribed to defects in RA, particularly the porous mortar adhering to Recycled Coarse Aggregate (RCA) and existing micro-cracks resulting from its crushing process. These factors contribute to a less compact matrix, consequently diminishing the concrete's strength. The enhancement of compressive strength, observed with 15% AAD and MOD, is influenced by microstructure refinement, the transformation of Calcium Hydroxide (CH) into Calcium Silicate Hydrate (CSH) gel through pozzolanic reactions, and the formation of a more condensed interfacial conversion zone. However, the replacement of 15% of cement by AAD and MOD led to a decline in concrete compressive strength. This decrease happened as a result of the concrete mixture's low SiO<sub>2</sub> level, which inhibited the development of C-S-H gel. Concrete's compressive strength is greatly influenced by C-S-H gel, which is largely produced by the interaction of CaO and SiO<sub>2</sub> in water [23].

#### 4.1.1. Split tensile strength

The STS outcomes of concrete featuring various levels of coarse aggregate replacement with recycled aggregate and cement substitution with AAD and MOD are illustrated in Figure 2. Examining the experimental data reveals that the highest splitting tensile strength occurs in mix RAMD03, achieved through 50% coarse aggregate replacement with recycled aggregate and 15% cement substitution by AAD and MOD. Moreover, it's evident that the splitting tensile strength rises with increasing AAD and MOD content, reaching a peak at 15%; however, beyond this point, the STS gradually diminishes. Elevation in concrete's tensile strength resulting from the replacement of 15% AAD and MOD is attributed to the notable densification of the concrete matrix. The unique characteristics of AAD and MOD, including their high surface area and chemical composition, contribute to enhancing concrete's tensile strength by reducing the transition zone between the binder paste and aggregates [18]. At the 15% replacement level of AAD and MOD, the porosity area fraction within the cement gel decreases due to the fine particle

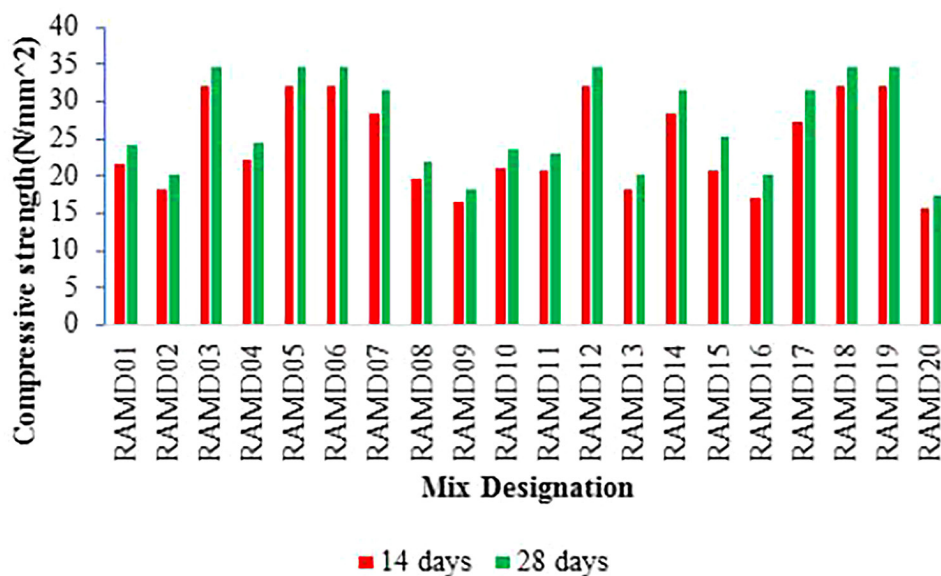


Figure 1: Compressive strength.

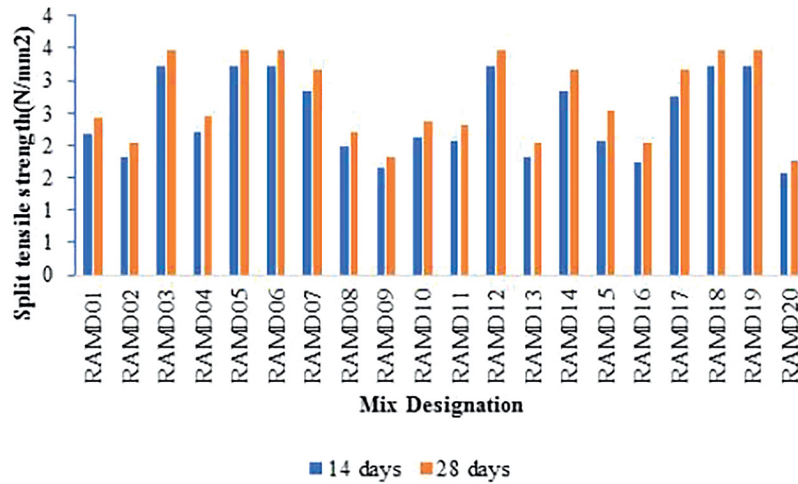


Figure 2: Split tensile strength.

size of AAD and MOD, leading to increased cement paste density. This increase ultimately enhances the concrete’s tensile strength.

#### 4.2. RSM Model

The study’s goal was to look into the influence of the variables Recycled aggregate ( $y_1$ ), Aluminium ash dross ( $y_2$ ) and Magnesium oxide dross ( $y_3$ ) on predicting the CS and STS of concrete mixes at fourteen and twenty eight and using the Central Composite Design. For this purpose, 20 trials were conducted for each retort, and the corresponding mix proportions are detailed in Table 2. The experimental outcomes were utilized to establish relationships concerning RA ( $y_1$ ), AAD ( $y_2$ ) and MOD ( $y_3$ ) resulting in the formulation of quadratic equations. The model equations, represented as Equation (1)–(3), are expressed in terms of coded factors.

$$fcs_{14} = 24.72 + 0.0917 y_1 + 0.430 y_2 + 0.585 y_3 - 0.001531 y_1^2 - 0.01667 y_2^2 - 0.01510 y_3^2 + 0.00147 y_1 * y_2 - 0.00084 y_1 * y_3 - 0.00762 y_2 * y_3 \quad (1)$$

$$fcs_{28} = 29.02 + 0.0715 y_1 + 0.343 y_2 + 0.599 y_3 - 0.001543 y_1^2 - 0.01581 y_2^2 - 0.01502 y_3^2 + 0.00241 y_1 * y_2 - 0.00101 y_1 * y_3 - 0.00885 y_2 * y_3 \quad (2)$$

$$fst_{14} = 2.472 + 0.00917 y_1 + 0.0430 y_2 + 0.0585 y_3 - 0.000153 y_1^2 - 0.001667 y_2^2 - 0.001510 y_3^2 + 0.000147 y_1 * y_2 - 0.000084 y_1 * y_3 - 0.000762 y_2 * y_3 \quad (3)$$

$$fst_{28} = 2.902 + 0.00715 y_1 + 0.0343 y_2 + 0.0599 y_3 - 0.000154 y_1^2 - 0.001581 y_2^2 - 0.001502 y_3^2 + 0.000241 y_1 * y_2 - 0.000101 y_1 * y_3 - 0.000885 y_2 * y_3 \quad (4)$$

Figure 3 illustrates that the residuals across all replies closely align with a straight line, indicating an even dispersion of errors. ANOVA, a statistical toolset, is employed to investigate the relationship between independent and dependent variables. The outcomes are summarized in Table 3 revealing that the models were highly appropriate as the lack-of-fit p-value was below 0.005. Furthermore, the models' predictions showed to be accurate, with a difference between predicted  $R^2$  and adjusted  $R^2$  for each response of less than 20%. The coefficient of determination ( $R^2$ ), gauging the fitness of the model, assesses how well the input parameters account for the measured response. Additionally, the relative  $R^2$  values for  $fcs_{14}$ ,  $fcs_{28}$ ,  $fst_{14}$ ,  $fst_{28}$  were 95.23%, 96.32%, 92.30%, and 96.23%, respectively. Table 4 showcases the correlation between predicted and experimental values, affirming the model's capability to forecast  $fcs_{14}$ ,  $fcs_{28}$ ,  $fst_{14}$ ,  $fst_{28}$ . The F value of the model, which validates its accuracy, is higher in cases where the F value is higher. Table 5 indicates F values of 20.44, 18.62, 20.64, and 18.62 for responses related to  $fcs_{14}$ ,  $fcs_{28}$ ,  $fst_{14}$ ,  $fst_{28}$ , respectively, affirming the robustness of the models.

**Table 3:** Observed and forecasted data acquired through RSM.

MIX DESIGNATION	COMPRESSIVE STRENGTH				SPLIT TENSILE STRENGTH			
	14 DAYS		28 DAYS		14 DAYS		28 DAYS	
	EXP	RSM	EXP	RSM	EXP	RSM	EXP	RSM
RAMD01	21.78	28.68	24.20	33.47	2.18	2.87	2.42	3.35
RAMD02	18.23	19.72	20.25	21.57	1.82	1.97	2.03	2.16
RAMD03	32.14	32.31	34.80	34.99	3.21	3.23	3.48	3.50
RAMD04	22.14	22.27	24.60	24.73	2.21	2.23	2.46	2.47
RAMD05	32.14	32.31	34.80	34.99	3.21	3.23	3.48	3.50
RAMD06	32.14	32.31	34.80	34.99	3.21	3.23	3.48	3.50
RAMD07	28.44	31.08	31.60	34.22	2.84	3.11	3.16	3.42
RAMD08	19.71	25.89	21.90	28.04	1.97	2.59	2.19	2.80
RAMD09	16.43	18.58	18.26	20.74	1.64	1.86	1.83	2.07
RAMD10	21.14	19.12	23.60	21.52	2.11	1.91	2.36	2.15
RAMD11	20.78	22.62	23.20	25.08	2.08	2.26	2.32	2.51
RAMD12	32.14	32.31	34.80	34.99	3.21	3.23	3.48	3.50
RAMD13	18.23	20.02	20.25	22.16	1.82	2.00	2.03	2.22
RAMD14	28.44	29.28	31.60	32.13	2.84	2.93	3.16	3.21
RAMD15	20.78	24.72	25.2	29.02	2.08	2.47	2.52	2.90
RAMD16	17.23	20.89	20.25	24.03	1.72	2.09	2.03	2.40
RAMD17	27.44	30.23	31.60	33.59	2.74	3.02	3.16	3.36
RAMD18	32.14	32.31	34.80	34.99	3.21	3.23	3.48	3.50
RAMD19	32.14	32.31	34.80	34.99	3.21	3.23	3.48	3.50
RAMD20	15.77	15.47	17.52	17.49	1.58	1.55	1.75	1.75

**Table 4:** ANOVA for  $fcs_{14}$ ,  $fcs_{28}$ ,  $fsts_{14}$  and  $fsts_{28}$ .

SOURCE	COMPRESSIVE STRENGTH $fcs_{14}$			COMPRESSIVE STRENGTH $fcs_{28}$			SPLIT TENSILE STRENGTH $fsts_{14}$			SPLIT TENSILE STRENGTH $fsts_{28}$		
	DF	F-VALUE	p-VALUE	DF	F-VALUE	p-VALUE	DF	F-VALUE	p-VALUE	DF	F-VALUE	p-VALUE
Model	9	6.23	0.004	9	5.75	0.006	9	6.23	0.004	9	5.75	0.006
Linear	3	2.64	0.107	3	3.31	0.065	3	2.64	0.107	3	3.31	0.065
$y_1$	1	5.36	0.043	1	6.11	0.033	1	5.36	0.043	1	6.11	0.033
$y_2$	1	1.64	0.229	1	2.29	0.161	1	1.64	0.229	1	2.29	0.161
$y_3$	1	0.92	0.361	1	1.53	0.244	1	0.92	0.361	1	1.53	0.244
Square	3	15.85	0.000	3	13.67	0.001	3	15.85	0.000	3	13.67	0.001
$y_1^2$	1	20.64	0.001	1	18.62	0.002	1	20.64	0.001	1	18.62	0.002
$y_2^2$	1	19.86	0.001	1	15.98	0.003	1	19.86	0.001	1	15.98	0.003
$y_3^2$	1	16.44	0.002	1	14.53	0.003	1	16.44	0.002	1	14.53	0.003
Two way interaction	3	0.20	0.894	3	0.26	0.850	3	0.20	0.894	3	0.26	0.850
$y_1 * y_2$	1	0.04	0.846	1	0.26	0.620	1	0.04	0.846	1	0.26	0.620
$y_1 * y_3$	1	0.04	0.846	1	0.10	0.759	1	0.04	0.846	1	0.10	0.759
$y_2 * y_3$	1	0.52	0.488	1	0.43	0.527	1	0.52	0.488	1	0.43	0.527

Table 5: Validation of test findings.

STRENGTH PROPERTIES	RA (%)	AAD (%)	MOD (%)	PREDICTED RESULT RSM	CONFIRMATION RESULTS
$fcs_{14}$	33.86	11.68	12.70	28.33	29.32
$fcs_{28}$	33.86	11.68	12.70	31.58	32.65
$fsts_{14}$	33.86	11.68	12.70	2.72	2.81
$fsts_{28}$	33.86	11.68	12.70	2.94	3.05

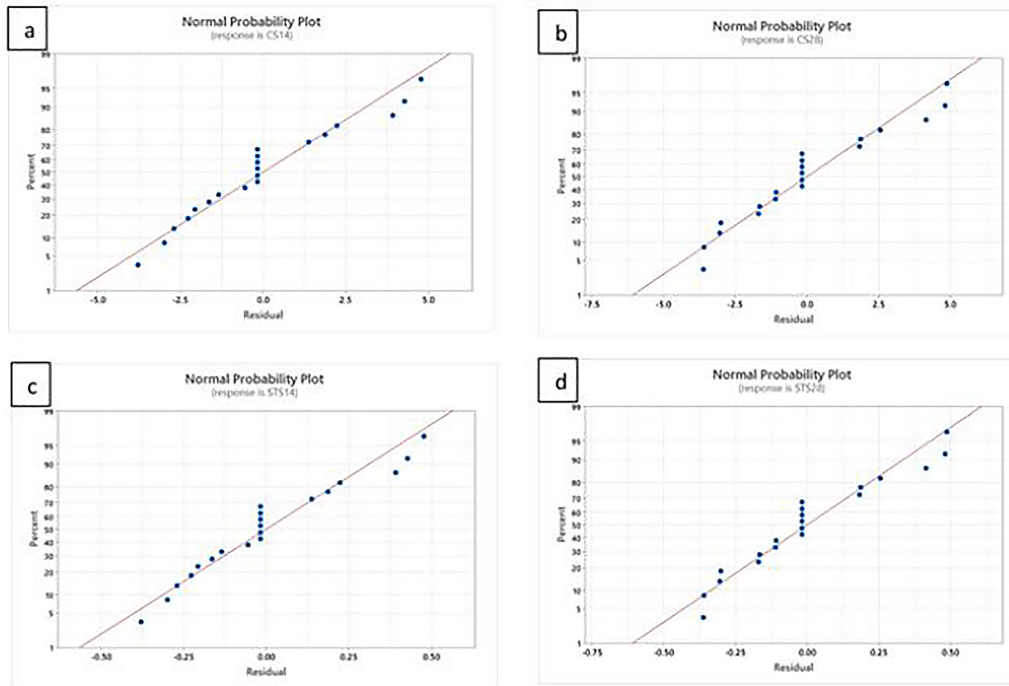


Figure 3: Normality probability graph a)  $fcs_{14}$ , b)  $fcs_{28}$ , c)  $fsts_{14}$ , and d)  $fsts_{28}$ .

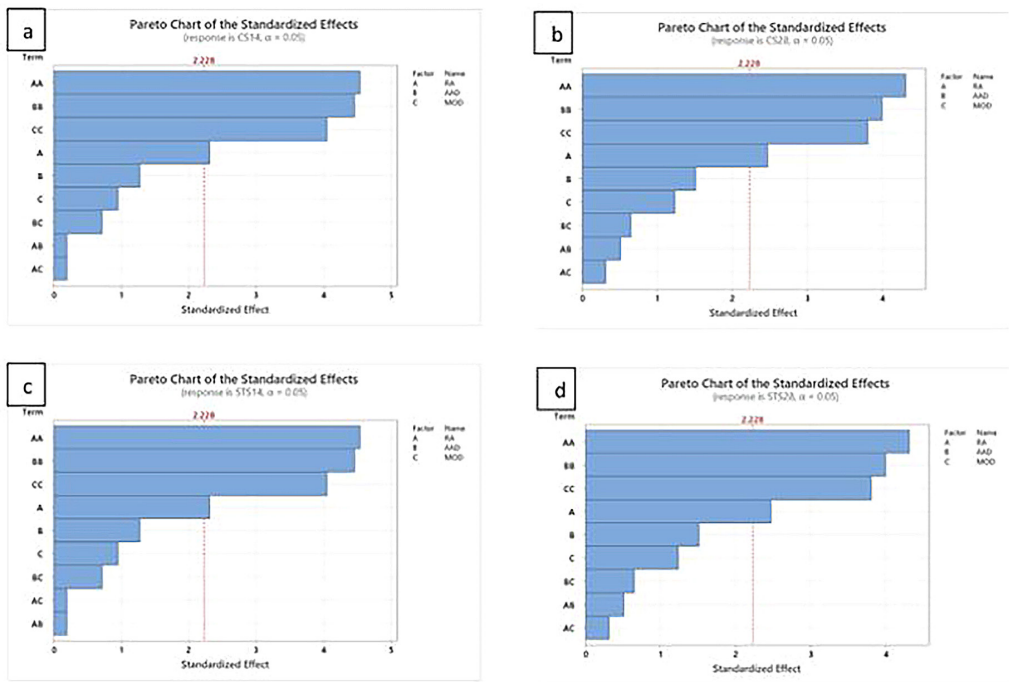


Figure 4: Pareto chart a)  $fcs_{14}$ , b)  $fcs_{28}$ , c)  $fsts_{14}$ , and d)  $fsts_{28}$ .

### 4.2.1. Pareto analysis and surface plot analysis

Assessing the importance of progression variables is facilitated by analysing the p-values. The p-value, indicative of the likelihood value of the F-test, is expected to be minimized, representing the model's significance. When independent variables possess p-values of 0.005 and 0.001, respectively, they signify considerable significance and substantial influence. If the progression variable's p-value is greater than 0.005, it's deemed insignificant. Table 5, utilizing ANOVA, highlights that the p-values of linear  $y_2$  and  $y_3$  were more than 0.005, while the p-values of  $y_1, y_1^2, y_2^2, y_3^2$  for  $fcs_{14}$  and  $fcs_{28}$  were under 0.005. The impact of AAD and MOD is minimal, evident from the p-values exceeding 0.005 for both linear  $y_2$  and  $y_3$ , affirming their limited influence on CS at 14 and 28 days. As depicted in Figures 4a and 4b via Pareto charts, Recycled aggregate takes precedence over Aluminium ash dross and Magnesium ash dross concerning compressive strength at both curing durations, with its value surpassing that of the other linears. Similarly, the ANOVA results in Table 4 indicate that for linear  $y_1$ , the p-value is lower compared to  $y_2$  and  $y_3$ , suggesting Recycled aggregate as a crucial factor in determining concrete compression strength. These findings align with prior research highlighting the substantial impact of adding recycled aggregate on compressive strength. However, recycled aggregate might significantly impact tensile strength in a

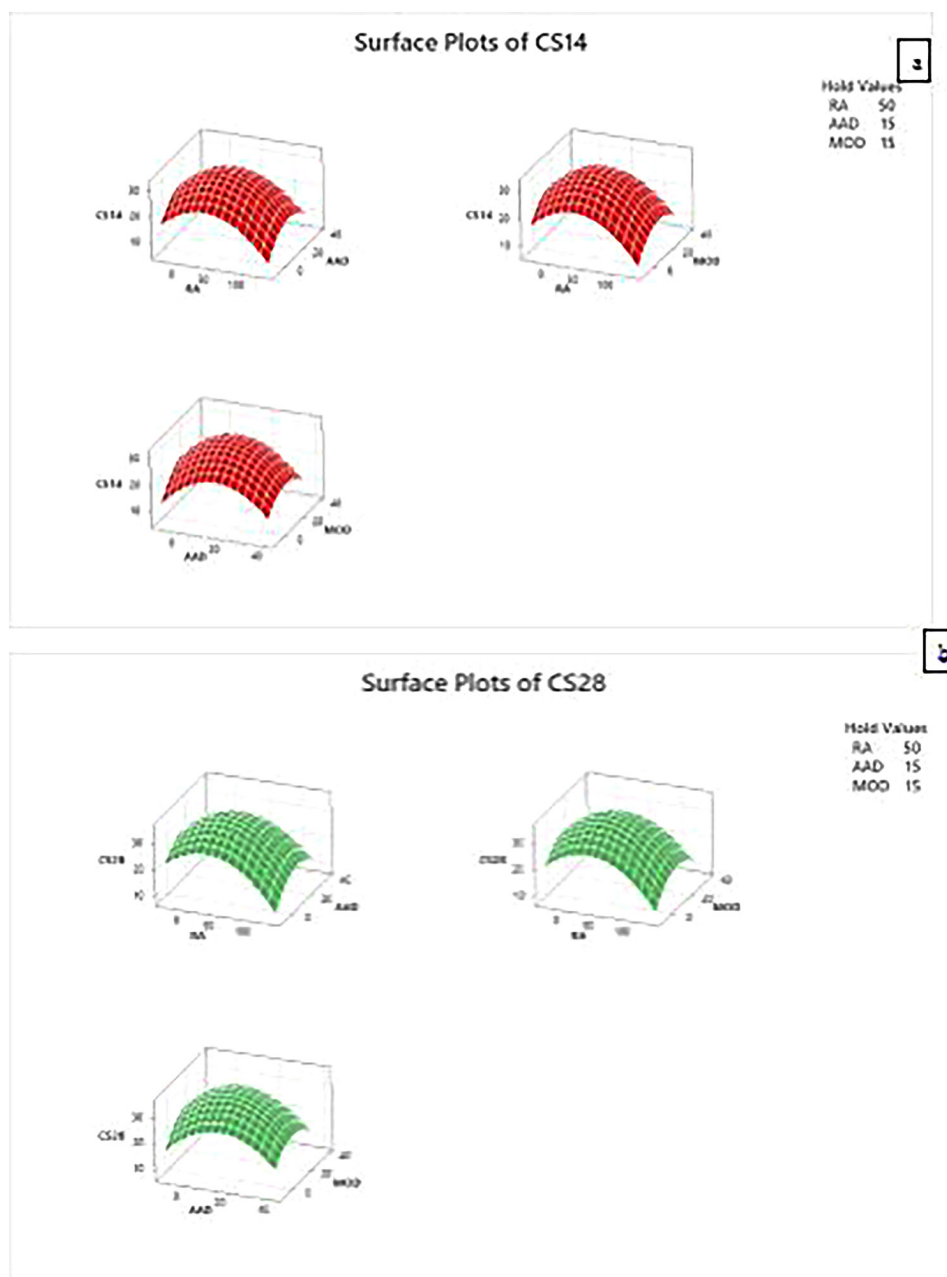


Figure 5: Contour plot a)  $fcs_{14}$ , b)  $fcs_{28}$ .



manner similar to its effect on compressive strength. When considering the STS at fourteen and twenty eight days, RA emerges as notably influential, contributing to the enhancement of tensile strength, with a p-value below 0.005. As indicated by Figures 5c and 5d, the impact of RA surpassed the standard values of 2.228 for both  $fsts_{14}$  and  $fsts_{28}$ . Additionally, the linear effect of RA (A) exhibited a greater influence when compared to (B & C). The increase in STS of concrete results from the grading effect created by the interplay among RA, AAD, and MOD in concrete compositions. Incorporating RA into concrete notably affects and augments both compressive and tensile strength qualities, as evidenced by the responses of  $fcs_{14}$ ,  $fcs_{28}$ ,  $fsts_{14}$ ,  $fsts_{28}$ .

Three-dimensional contour plots intended to clarify how progression variables affect the results are shown in Figures 5 and 6. The response is depicted along the 'z' axis of the surface plot, while the progression variables (RA, AAD, and MOD) are charted along the 'x' and 'y' directions. Figure 5 illustrates that a composition featuring 50% Recycled aggregate, 15% Aluminium ash dross, and 15% Magnesium oxide dross yields the highest CS at fourteen and twenty eight days of curing, respectively.

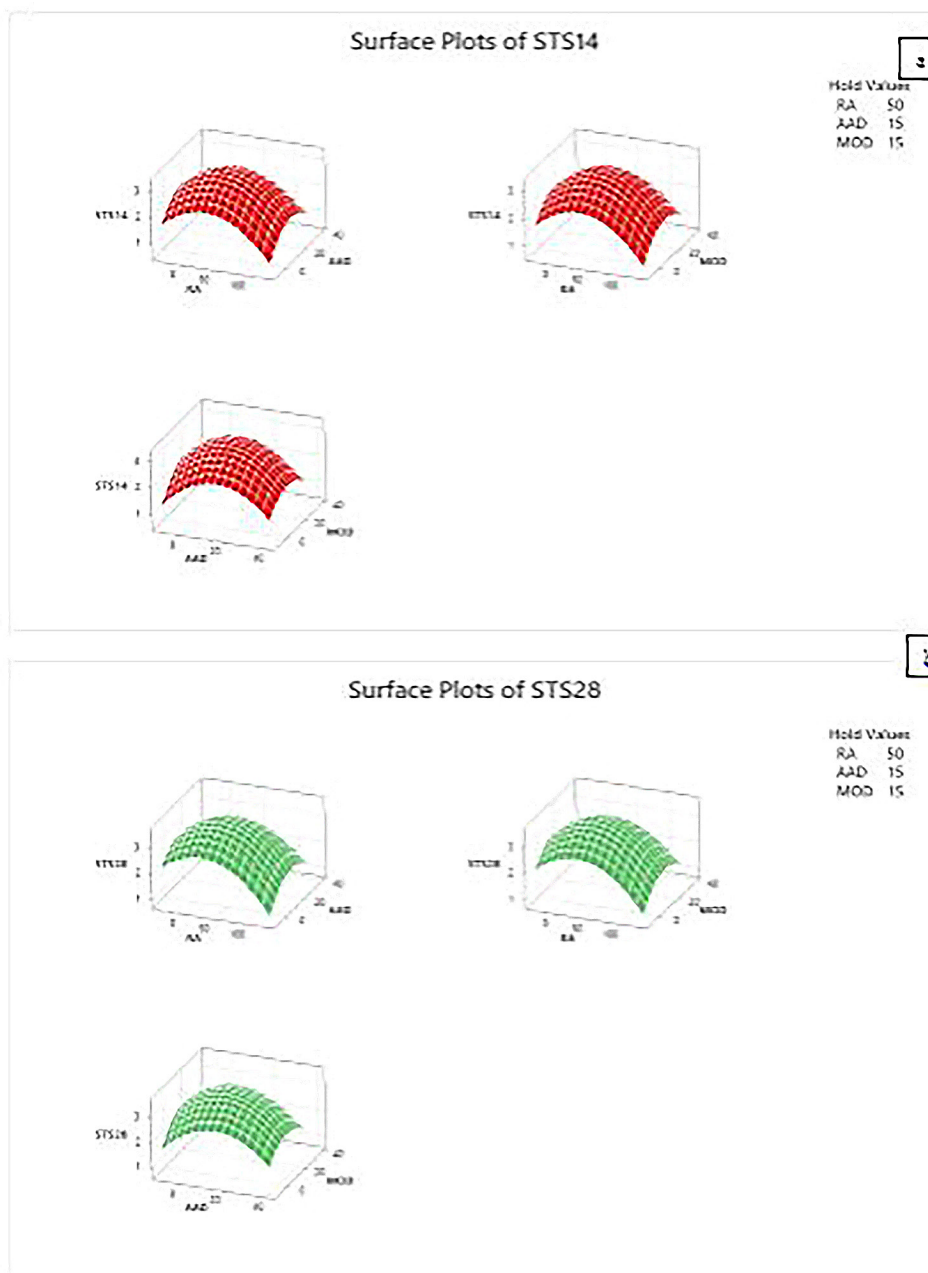


Figure 6: Contour plot a)  $fsts_{14}$ , b)  $fsts_{28}$ .

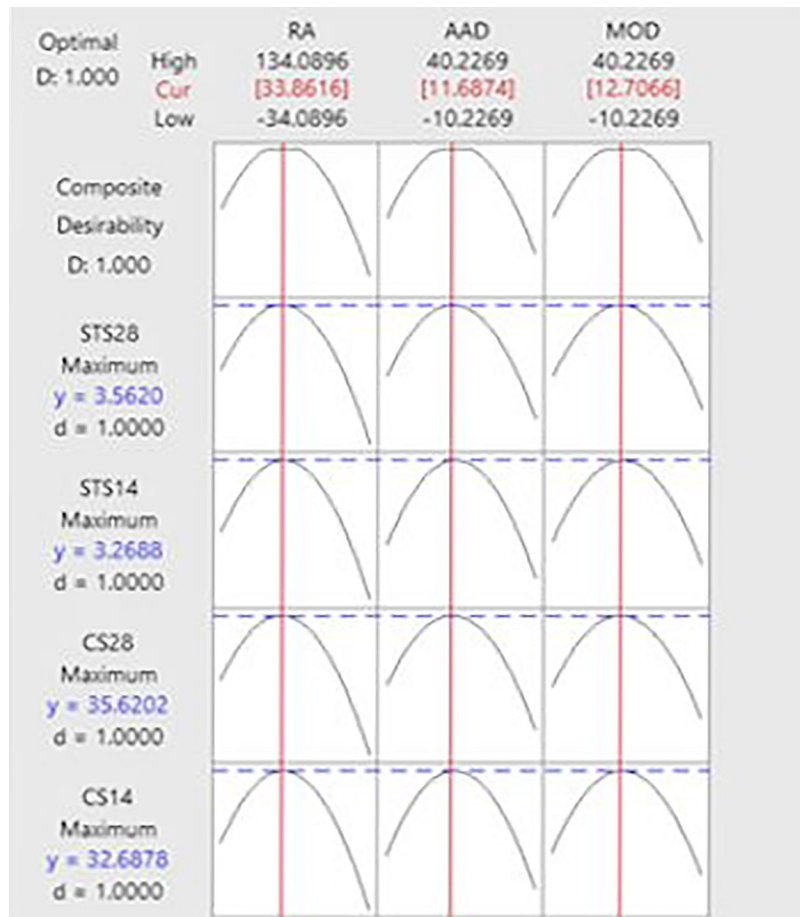


Figure 7: Optimisation chart  $fcs_{14}, fcs_{28}, fst_{14}, fst_{28}$ .

However, beyond the 50% threshold for Recycled aggregate, the strength diminishes. While the addition of Recycled aggregate contributes to increased compressive strength in concrete, Aluminium ash dross and Magnesium ash dross wield significant influence during the 14 and 28-day curing phases. The optimization of progression variables reveals that exceeding 50% substitution of coarse aggregate with Recycled Aggregate (RA) results in a reduction in compressive strength. The highest compressive strength values for  $fcs_{14}$  and  $fcs_{28}$  were achieved with a concrete mix comprising 50% RA, 15% Aluminium Ash Dross (AAD), and 15% Magnesium Oxide Dross (MOD). As depicted in Figure 6, augmenting the RA content corresponds to an increase in tensile strength for both  $fst_{14}$  and  $fst_{28}$ , highlighting RA's substantial impact on enhancing STS. Moreover, the tensile strength of concrete diminishes as the weight fraction exceeds a certain limit.

### 4.3. Optimization of progression variables

As per Figure 7, the optimal proportions of RA, AAD, and MOD to achieve peak CS and STS at both 14 and 28 days were 33.86%, 11.68%, and 12.70%, respectively. A validation test was conducted to substantiate these findings, as showcased in Table 5. The results in Table 5 indicate that the predicted results of RSM are similar to experimental findings of  $fcs_{14}, fcs_{28}, fst_{14}$ , and  $fst_{28}$ .

## 5. CONCLUSION

After employing the CCD of RSM to optimize the strength characteristics of concrete involving RA, AAD, and MOD, the subsequent results were obtained:

1. The incorporation of recycled aggregates (RA) at a 50% rate has improved the CS characteristics of concrete. Furthermore, the test outcomes suggest that surpassing a 50% addition of RA leads to a reduction in compressive strength.

2. The addition of AAD and MOD in concrete has led to slight enhancements in both its compressive and split tensile strength. Nonetheless, it is important to highlight that as the levels of AAD and MOD increase, the strength diminishes.
3. The regression analysis model created for forecasting  $f_{cs_{14}}$ ,  $sfsts_{14}$  and  $fsts_{28}$  exhibits a strong correlation between the predicted values and the outcomes obtained through experimentation.
4. The outcomes of the ANOVA reveal that Recycled aggregate stood out as the most significant factor impacting both the fourteen and twenty eight days CS and STS of the concrete.
5. The design parameters that resulted in the best outcomes for  $f_{cs_{14}}$ ,  $f_{cs_{28}}$ ,  $fsts_{14}$ , and  $fsts_{28}$  were attained, highlighting their substantial importance in concrete design.
6. The Pareto chart analysis and ANOVA demonstrated the significant relevance of the developed models for  $f_{cs_{14}}$ ,  $sfsts_{14}$  and  $fsts_{28}$ . These models showcased remarkable accuracy, supported by the p-values below 0.005.

## 6. BIBLIOGRAPHY

- [1] PATRA, I., AL-AWSI, G.R.L., HASAN, Y.M., *et al.*, “Mechanical properties of concrete containing recycled aggregate from construction waste”, *Sustainable Energy Technologies and Assessments*, v. 53, pp. 102722, Oct. 2022. doi: <http://doi.org/10.1016/j.seta.2022.102722>.
- [2] MAILAR, G., SREEDHARA, B.M., MANU, D.S., *et al.*, “Investigation of concrete produced using recycled aluminium dross for hot weather concreting conditions”, *Resource-Efficient Technologies*, v. 2, n. 2, pp. 68–80, 2016. doi: <http://doi.org/10.1016/j.refit.2016.06.006>.
- [3] ARASU, N., RAFSAL, M.M., SURYA KUMAR, O.R., “Experimental investigation of high performance concrete by partial replacement of fine aggregate by construction demolition waste”, *International Journal of Scientific and Engineering Research*, v. 9, n. 3, 2018.
- [4] KADHAR, S.A., GOPAL, E., SIVAKUMAR, V., *et al.*, “Optimizing flow, strength, and durability in high-strength self-compacting and self-curing concrete utilizing lightweight aggregates”, *Matéria (Rio de Janeiro)*, v. 29, n. 1, pp. e20230336, 2024. doi: <http://doi.org/10.1590/1517-7076-rmat-2023-0336>.
- [5] PEDRO, D., DE BRITO, J., EVANGELISTA, L., “Structural concrete with simultaneous incorporation of fine and coarse recycled concrete aggregates: mechanical, durability and long-term properties”, *Construction & Building Materials*, v. 154, pp. 294–309, Nov. 2017. doi: <http://doi.org/10.1016/j.conbuildmat.2017.07.215>.
- [6] NAVEEN ARASU, A., NATARAJAN, M., BALASUNDARAM, N., *et al.*, “Optimization of high performance concrete by using nano materials”, *Research on Engineering Structures Materials*, v. 3, n. 9, pp. 843–859, 2023.
- [7] PARTHASAARATHI, R., BALASUNDARAM, N., ARASU, N., “Analysing the impact and investigating Coconut Shell Fiber Reinforced Concrete (CSFRC) under varied loading conditions”, *Journal of Advanced Research in Applied Sciences and Engineering Technology*, v. 35, n. 1, pp. 106–120, 2024.
- [8] DABIRI, H., KIOUMARSI, M., KHEYRODDIN, A., *et al.*, “Compressive strength of concrete with recycled aggregate, a machine learning-based evaluation”, *Cleaner Materials*, v. 3, pp. 100044, Mar. 2022. doi: <http://doi.org/10.1016/j.clema.2022.100044>.
- [9] HADAVAND, B., IMANINASAB, R., “Assessing the influence of construction and demolition waste materials on workability and mechanical properties of concrete using statistical analysis”, *Innovative Infrastructure Solutions*, v. 4, n. 1, pp. 1–11, 2019. doi: <http://doi.org/10.1007/s41062-019-0214-3>.
- [10] CARNEIRO, J.A., LIMA, P.R.L., LEITE, M.B., *et al.*, “Compressive stress-strain behavior of steel fiber reinforced-recycled aggregate concrete”, *Cement and Concrete Composites*, v. 46, pp. 65–72, Feb. 2014. doi: <http://doi.org/10.1016/j.cemconcomp.2013.11.006>.
- [11] ZHENG, C., LOU, C., DU, G., *et al.*, “Mechanical properties of recycled concrete with demolished waste concrete aggregate and clay brick aggregate”, *Results in Physics*, v. 9, pp. 1317–1322, Jun. 2018. doi: <http://doi.org/10.1016/j.rinp.2018.04.061>.
- [12] NANAYAKKARA, O., GUNASEKARA, C., LAW, D.W., *et al.*, “Alkali-activated slag concrete with recycled aggregate: long-term performance”, *Journal of Materials in Civil Engineering*, v. 33, n. 7, pp. 04021167, Jul. 2021. doi: [http://doi.org/10.1061/\(ASCE\)MT.1943-5533.0003773](http://doi.org/10.1061/(ASCE)MT.1943-5533.0003773).

- [13] ARORA, S., SINGH, S., “Flexural fatigue performance of concrete made with recycled concrete aggregates and ternary blended cements”, *Journal of Sustainable Cement-Based Materials*, v. 7, n. 3, pp. 182–202, May 2018. doi: <http://doi.org/10.1080/21650373.2018.1471423>.
- [14] MOHAMMED, D., TOBEIA, S., MOHAMMED, F., *et al.*, “Compressive strength improvement for recycled concrete aggregate”, In: *MATEC Web of Conferences*, v. 162, pp. 02018, 2018. doi: <http://doi.org/10.1051/mateconf/201816202018>.
- [15] XIAO, J., LI, J., ZHANG, C., “Mechanical properties of recycled aggregate concrete under uniaxial loading”, *Cement and Concrete Research*, v. 35, n. 6, pp. 1187–1194, Jun. 2005. doi: <http://doi.org/10.1016/j.cemconres.2004.09.020>.
- [16] ELSEKNIDY, M.H., SALMIATON, A., NOR SHAFIZAH, I., *et al.*, “A study on mechanical properties of concrete incorporating aluminum dross, fly ash, and quarry dust”, *Sustainability (Basel)*, v. 12, n. 21, pp. 9230, Nov. 2020. doi: <http://doi.org/10.3390/su12219230>.
- [17] RAMAKRISHNAN, S., NICOLAU JUNIOR, D.V., LANGFORD, B., *et al.*, “Inhaled budesonide in the treatment of early COVID-19 (STOIC): a phase 2, open-label, randomised controlled trial”, *The Lancet. Respiratory Medicine*, v. 9, n. 7, pp. 763–772, 2021. doi: [http://doi.org/10.1016/S2213-2600\(21\)00160-0](http://doi.org/10.1016/S2213-2600(21)00160-0). PubMed PMID: 33844996.
- [18] MAILAR, G., SREEDHARA, B.M., MANU, D.S., *et al.*, “Investigation of concrete produced using recycled aluminium dross for hot weather concreting conditions”, *Resource-Efficient Technologies*, v. 2, n. 2, pp. 68–80, 2016. doi: <http://doi.org/10.1016/j.reffit.2016.06.006>.
- [19] NDUKA, D.O., JOSHUA, O., AJAO, A.M., *et al.*, “Influence of secondary aluminum dross (SAD) on compressive strength and water absorption capacity properties of sandcrete block”, *Cogent Engineering*, v. 6, n. 1, pp. 1608687, Jan. 2019. doi: <http://doi.org/10.1080/23311916.2019.1608687>.
- [20] GANAPATHY, G.P., ALAGU, A., RAMACHANDRAN, S., *et al.*, “Effects of fly ash and silica fume on alkalinity, strength and planting characteristics of vegetation porous concrete”, *Journal of Materials Research and Technology*, v. 24, pp. 5347–5360, May 2023. doi: <http://doi.org/10.1016/j.jmrt.2023.04.029>.
- [21] THIRUKUMARAN, T., KRISHNAPRIYA, S., PRIYA, V., *et al.*, “Utilizing rice husk ash as a bio-waste material in geopolymer composites with aluminium oxide”, *Global NEST Journal*, v. 25, n. 6, pp. 119–129, 2023.
- [22] ARASU, N.A., RAMASAMY, V.P., HARVEY, D.V., “A experimental analysis on bio concrete with bentonite as partial replacement of cement”, *International Research Journal of Engineering and Technology*, v. 7, n. 10, pp. 689–695, 2020.
- [23] ARASU, A.N., NATARAJAN, M., BALASUNDARAM, N., *et al.*, “Development of high-performance concrete by using nanomaterial graphene oxide in partial replacement for cement”, In: *AIP Conference Proceedings*, vol. 2861, 2023. doi: <http://doi.org/10.1063/5.0158487>.